


Cite this: *RSC Adv.*, 2025, **15**, 27551

Received 11th May 2025  
Accepted 23rd July 2025

DOI: 10.1039/d5ra03301b  
rsc.li/rsc-advances

## Mild synthesis of fused polycyclic 1,6-naphthyridin-4-amines and their optical properties

Ze Li,<sup>ab</sup> Dongfeng Zhang, Hanxun Wang, Haihong Huang,<sup>\*b</sup> Maosheng Cheng <sup>\*a</sup> and Hongyi Zhao <sup>\*b</sup>

A mild and straightforward synthetic route to tri-, tetra-, and pentacyclic 1,6-naphthyridin-4-amines is presented. The protocol involves  $\text{CF}_3\text{SO}_3\text{H}$ - or  $\text{H}_2\text{SO}_4$ -mediated Friedel-Crafts-type intramolecular cycloaromatisation of 4-(arylamino)nicotinonitriles in which the cyano group acts as a one-carbon synthon. The transformation achieves good to excellent yields and can be performed on a gram scale. Additionally, the exploration of fluorescence properties of these compounds demonstrates their potential application as fluorophores.

### Introduction

The 1,6-naphthyridine scaffold is widely found in natural products<sup>1</sup> and pharmaceutical molecules.<sup>2</sup> Among them, benzo[1,6]naphthyridines exhibit a wide range of bioactivities, including inhibition activity against MAO B,<sup>3</sup> PDE5,<sup>4</sup> BTK,<sup>5</sup> Topo I,<sup>6</sup> hAChE,<sup>7</sup> and noradrenaline uptake,<sup>8</sup> as well as antimalarial activity.<sup>9</sup> Some fused polycyclic 1,6-naphthyridines also exhibit interesting optical and/or electrochemical properties,<sup>10</sup> making them promising as organic luminescence materials and probes (Fig. 1). Accordingly, numerous diverse synthetic strategies have been developed for the construction of these structurally complex molecules.<sup>2,11</sup>

The emerging bioactivity profile of benzo[1,6]naphthyridin-4-amine derivatives observed in our recent studies prompts us to develop their synthetic methodology for scaffold diversification. Literature analysis reveals that acid-mediated intramolecular Friedel-Crafts reactions serve as an important strategy for the synthesis of the benzo[1,6]naphthyridine scaffold. However, the ring-closure strategies typically rely on the presence of an aldehyde,<sup>12</sup> ketone,<sup>13</sup> or carboxylic acid<sup>14</sup> moiety at the ortho-position of the aniline to serve as a one-carbon synthon (Scheme 1), and the functional groups generated upon ring closure provide limited options for later-stage derivatization. Additionally, most of these established methods necessitate elevated temperature to achieve dehydration and cyclisation except for a few mild protocols,<sup>13c,d</sup> and they are

inefficient means of synthesising the benzo[1,6]naphthyridin-4-amine scaffold because the cyclisation product requires further functional-group conversion to generate the amino group. To the best of our knowledge, limited attention has been paid to the mild and straightforward access to the fused polycyclic 1,6-naphthyridin-4-amines. Therefore, the application of a new one-carbon synthon coupled with the establishment of a mild, direct synthetic protocol for diverse benzo[1,6]naphthyridin-4-amine derivatives would be highly desirable.

McKenna *et al.* first reported the construction of the benzo[1,6]naphthyridin-4-amine scaffold<sup>8</sup> *via* a  $\text{BF}_3 \cdot \text{Et}_2\text{O}$ -mediated Friedländer<sup>15</sup> annulation between anthranilonitrile and 4-oxo-

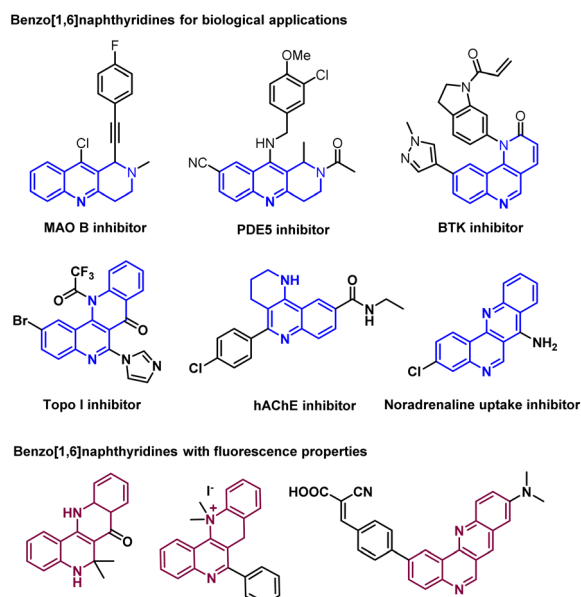


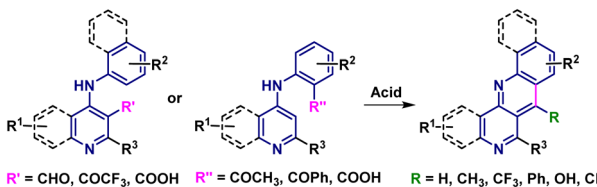
Fig. 1 Examples of biologically active and fluorescent polycyclic benzo[1,6]naphthyridines.

<sup>a</sup>Key Laboratory of Structure-Based Drug Design & Discovery of Ministry of Education, School of Pharmaceutical Engineering, Shenyang Pharmaceutical University, Shenyang 110016, Liaoning, P. R. China. E-mail: mscheng@syphu.edu.cn

<sup>b</sup>Beijing Key Laboratory of Active Substance Discovery and Druggability Evaluation, Chinese Academy of Medical Sciences Key Laboratory of Anti-DR TB Innovative Drug Research, Institute of Materia Medica, Peking Union Medical College and Chinese Academy of Medical Sciences, 1 Xian Nong Tan Street, Beijing, 100050, P. R. China. E-mail: joyce@imm.ac.cn; zhaohongyicool@imm.ac.cn



## a) Previous work (aldehyde, ketone or carboxylic acid as the one-carbon synthons)



## b) This work (cyano group as the one-carbon synthon)



Scheme 1 Synthesis of benzo[1,6]naphthyridine derivatives from precursors with different one-carbon synthons.

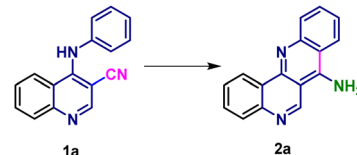
7-chloro-1,2,3,4-tetrahydroquinoline, achieving a yield of 21%. In addition, the cyano group has emerged as an efficient one-carbon synthon in the construction of functionalised 4-aminoquinolines and their fused-cyclic analogues through nitrile-activation strategies.<sup>16</sup> These studies inspired us to explore the synthesis of fused polycyclic 1,6-naphthyridin-4-amines *via* a cyano-based intramolecular Friedel–Crafts annulation strategy. Accordingly, we herein report a mild and effective method for accessing fused polycyclic 1,6-naphthyridin-4-amine derivatives *via* CF<sub>3</sub>SO<sub>3</sub>H- or H<sub>2</sub>SO<sub>4</sub>-mediated cycloaromatisation of 4-(arylamino)nicotinonitrile precursors. Additionally, the fluorescence properties of the products were investigated.

## Results and discussion

### Chemistry

Initially, 4-(phenylamino)quinoline-3-carbonitrile (**1a**) was chosen as a model substrate to establish and optimise the reaction conditions (Table 1). Upon treatment in pure CF<sub>3</sub>SO<sub>3</sub>H at room temperature for 0.5 h, the desired tetracyclic compound **2a** was obtained in 84% yield (entry 1). We next screened other acids (entries 2–4), showing that pure H<sub>2</sub>SO<sub>4</sub> also promotes the annulation in 82% yield (entry 2). To optimise the cyclisation condition, CF<sub>3</sub>SO<sub>3</sub>H solutions in various solvents were evaluated to identify the optimal solvent system (entries 5–9). A remarkable solvent effect was observed. The reaction did not proceed adequately in DMSO, acetone, CH<sub>3</sub>CN and DMF. However, when the reaction was conducted in DCM solution, a comparable yield (entry 9) to that obtained with pure CF<sub>3</sub>SO<sub>3</sub>H (entry 1) was achieved. Considering the high cyclisation effect of pure H<sub>2</sub>SO<sub>4</sub>, a mixture of DCM and concentrated H<sub>2</sub>SO<sub>4</sub> was evaluated and afforded **2a** in 89% yield (entry 10). However, it was ultimately discovered to be a biphasic solvent system, making it a less desirable choice due to the potential temperature control risks. Accordingly, the optimal reaction conditions were established to be: **1a** (0.1 g), CF<sub>3</sub>SO<sub>3</sub>H (10 equiv.), CH<sub>2</sub>Cl<sub>2</sub> (3 mL), room temperature, 0.5 h (entry 9).

Table 1 Optimisation of reaction conditions<sup>a</sup>



| Entry | Acid  | Solvent | t (h) | Yield <sup>b</sup> (%) |
|-------|---|---------|-------|------------------------|
| 1     | CF <sub>3</sub> SO <sub>3</sub> H (1.5 mL)    | —       | 0.5   | 84                     |
| 2     | H <sub>2</sub> SO <sub>4</sub> (1.5 mL)       | —       | 0.5   | 82                     |
| 3     | CH <sub>3</sub> SO <sub>3</sub> H (1.5 mL)    | —       | 2     | Trace                  |
| 4     | CF <sub>3</sub> COOH (1.5 mL)                 | —       | 10    | ND <sup>c</sup>        |
| 5     | CF <sub>3</sub> SO <sub>3</sub> H (10 equiv.) | DMSO    | 5.5   | Trace                  |
| 6     | CF <sub>3</sub> SO <sub>3</sub> H (10 equiv.) | Acetone | 5.5   | Trace                  |
| 7     | CF <sub>3</sub> SO <sub>3</sub> H (10 equiv.) | MeCN    | 5.5   | Trace                  |
| 8     | CF <sub>3</sub> SO <sub>3</sub> H (10 equiv.) | DMF     | 2     | ND <sup>c</sup>        |
| 9     | CF <sub>3</sub> SO <sub>3</sub> H (10 equiv.) | DCM     | 0.5   | 92                     |
| 10    | H <sub>2</sub> SO <sub>4</sub> (10 equiv.)    | DCM     | 0.5   | 89                     |

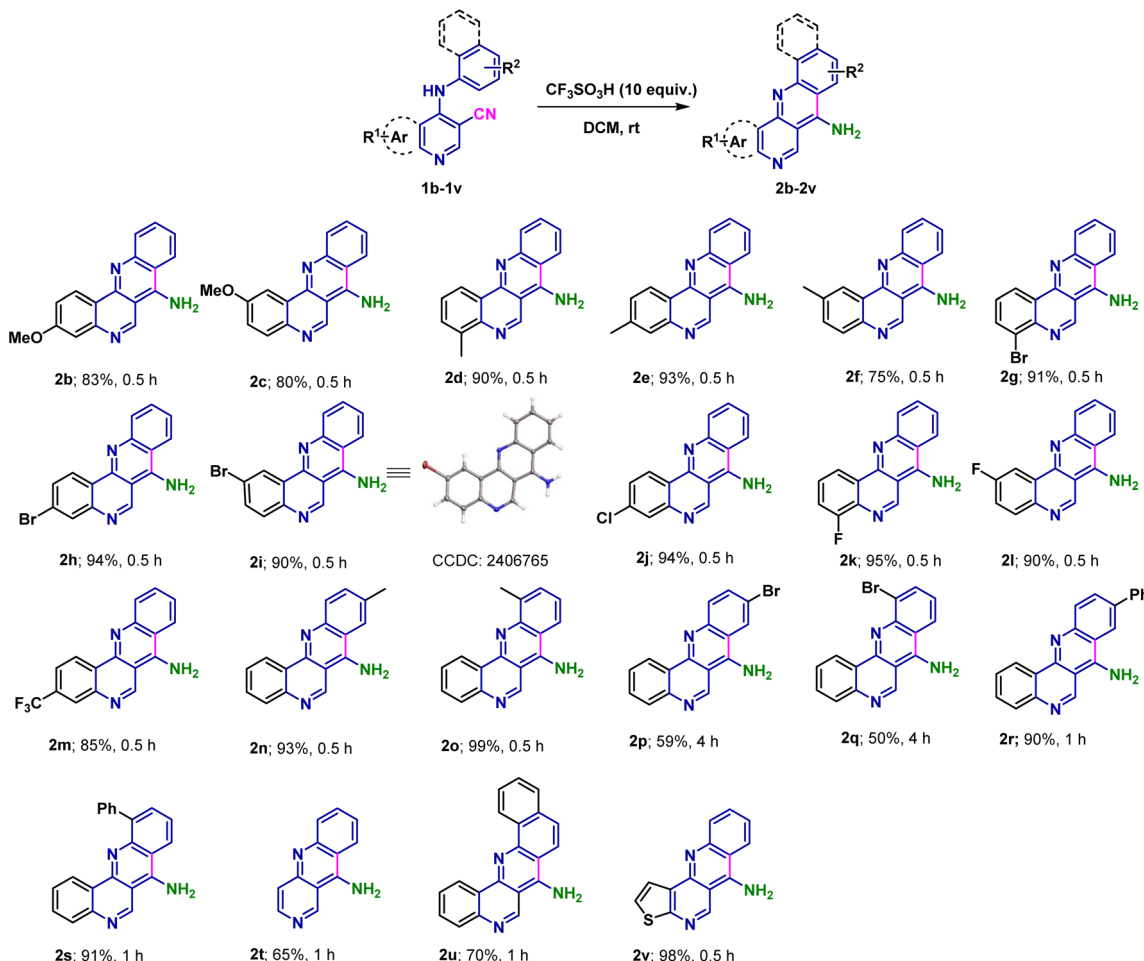
<sup>a</sup> Reaction conditions: **1a** (0.1 g), acid (1.5 mL or 10 equiv. in 3 mL solvent), rt. <sup>b</sup> Isolated yields. <sup>c</sup> ND = not detected.

Having established the optimised reaction conditions, the substrate scope for substituted 4-(arylamino)nicotinonitriles **1** was evaluated. As shown in Scheme 2, annulated polycyclic compounds **2b–2v** were obtained in moderate to excellent yields. The choice of substituent on the benzene ring of the quinoline moiety had negligible impact on reactivity, with substrates bearing both electron-donating (OMe, Me) and electron-withdrawing groups (Br, Cl, F, CF<sub>3</sub>) on that ring affording the desired products **2b–2m** in good to excellent yields (75–95%). Furthermore, compound **2j** was obtained in a much higher yield (94% *vs.* 21%) than that reported previously.<sup>8</sup> Compounds **2n** and **2o** bearing a methyl group on the aniline moiety were generated in 93% and 99% yields, respectively, while products **2p** and **2q** bearing an electronegative bromine atom were obtained in moderate yields (50% and 59%) due to incomplete consumption of starting materials, even after extending the reaction time to 4 hours. This indicates that an electron-withdrawing group on the aniline hinders the progress of the reaction, which is also consistent with the mechanistic framework of the Friedel–Crafts reaction. Additionally, the phenyl-substituent products **2r** and **2s** were obtained in excellent yields in 1 h.

Gratifyingly, benzo[*b*][1,6]naphthyridin-10-amine (**2t**), benzo[*h*]naphtho[1,2-*b*]naphthyridin-7-amine (**2u**), and benzo[*b*]thieno[2,3-*h*]naphthyridin-6-amine (**2v**) were synthesised in 65%, 70%, and 98% yields, respectively, demonstrating the broad accessibility to fused heterocyclic structures available with this protocol. Finally, the structure of **2i** was unambiguously established by X-ray crystallographic analysis (CCDC: 2406765), confirming its planar structure.

Encouraged by our results showing that efficient annulation can be also mediated by H<sub>2</sub>SO<sub>4</sub> (Table 1), we explored whether the moderate yields achieved using CF<sub>3</sub>SO<sub>3</sub>H with substrates bearing electron-withdrawing groups on the aniline moiety



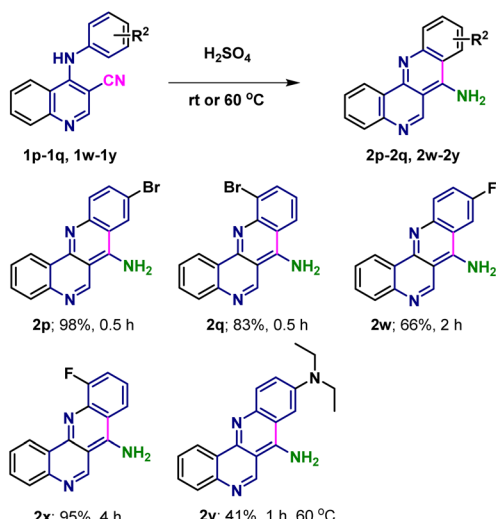
Scheme 2 Synthesis of products 2b–2v using  $\text{CF}_3\text{SO}_3\text{H}$  in DCM solution.

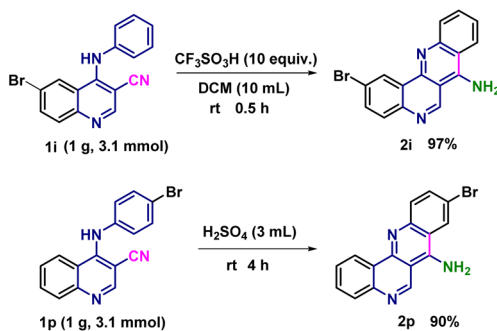
could be enhanced by employing concentrated  $\text{H}_2\text{SO}_4$  as the cyclising agent (Scheme 3). Subsequently, **1p** and **1q** were successfully converted into products **2p** and **2q** in 98% and 83%

yields, respectively, after 0.5 h. Furthermore, substrates **1w** and **1x** bearing a fluorine on the aniline moiety successfully delivered the tetracyclic heteroaromatics **2w** and **2x** in 66% and 95% yields, respectively. However, diethylamino-substituted substrate **1y** did not react under standard conditions or in pure  $\text{H}_2\text{SO}_4$  at ambient temperature. Rather, its successful annulation required elevated temperature ( $60^\circ\text{C}$ ), ultimately affording **2y** in 41% yield after column chromatography. This marked difference in reactivity is likely due to sulfate formation by the diethylamino group, generating a strong electron-withdrawing effect that impedes annulation at the cyano group.

Collectively, these results indicate that concentrated  $\text{H}_2\text{SO}_4$  effectively facilitates cyclisation of substrates bearing electron-withdrawing substituents on the aniline moiety.

To demonstrate the excellent scalability of the present protocol, gram-scale preparations of compounds **2i** and **2p** were performed from precursor **1i** (1 g, 3.1 mmol) and **1p** (1 g, 3.1 mmol), respectively, using the two sets of acidic conditions established above. To reduce the proportion of solvent or sulfuric acid usage, the volume of dichloromethane was decreased during the preparation of **2i**, and the amount of sulfuric acid was reduced during the synthesis of **2p**. Both reactions maintained high yields, delivering the target

Scheme 3 Annulation of substrates bearing electron-withdrawing substituents on the aniline moiety in concentrated  $\text{H}_2\text{SO}_4$ .

Scheme 4 Gram-scale preparation of **2i** and **2p**.

compounds in yields of 97% and 90%, respectively (Scheme 4). The scaled-up synthesis demonstrated the mildness and convenience of the protocol in this study.

### Photophysical evaluation

Fused 1,6-naphthyridine derivatives have attracted significant research attention owing to their intriguing optical and electrochemical properties.<sup>10</sup> Accordingly, we conducted absorption and fluorescence emission spectral analysis of these tri-, tetra-, and pentacyclic compounds in dilute DMSO solutions ( $1 \times 10^{-5}$  mol L<sup>-1</sup>).

As shown in Table 2, the absorption spectra of the 1,6-naphthyridine-4-amine derivatives show multiple overlapping broad bands with maximum absorption wavelengths ranging from 344 to 448 nm (see the SI). The maximum absorption wavelengths of most tetracyclic compounds (**2a**–**2s**, **2w**, **2x**) are concentrated in the range of 344–428 nm. Notably, compound **2y** bearing the auxochromic diethylamino substituent exhibits a bathochromic shift in its maximum absorption wavelength, reaching 448 nm. The tricyclic compound **2t** displays a red-shift, while the pentacyclic compound **2u** undergoes a hypsochromic shift. The sulfur-containing tetracyclic compound **2v** also demonstrates a red-shift. For representative tri-, tetra-, and pentacyclic compounds (**2a**, **2t**, **2u**, **2v**, and **2y**), we computed their vertical excitation energies using Gaussian calculations (Table S2). The results are as follows: **2a** (3.291 eV), **2t** (3.156 eV), **2u** (3.261 eV), **2v** (3.098 eV), and **2y** (2.716 eV). The computational results are consistent with the observed direction of wavelength shifts. Regarding the influence on molar absorption coefficients ( $\epsilon$ ), most compounds exhibit strong absorption characteristics ( $\epsilon \geq 4273 \text{ M}^{-1} \text{ cm}^{-1}$ ), while compounds **2t**, **2v**, and **2w** demonstrate weaker absorption. Among compounds **2d**–**2l**, compounds **2d**, **2g**, and **2k** display much higher  $\epsilon$ , particularly the halogen-substituted compounds **2g** and **2k**. Furthermore, compounds **2r**, **2s**, and **2u** with extended conjugation systems manifest a hyperchromic effect.

The fluorescence emission spectra recorded under 365 nm excitation show that most of the compounds present maximum emission peaks around 450 nm. It should be additionally noted that compound **2b** exhibits a red-shifted emission wavelength at 460 nm compared to **2a** and **2c**, indicating that the strong electron-donating at the 3-position is critical for the red-shift. Additionally, benzene-substituted compounds **2r** and **2s** also

Table 2 Photophysical properties of the tricyclic, tetracyclic, and pentacyclic 1,6-naphthyridin-4-amine compounds

| Compd     | $\lambda_{\text{abs}}^a$ (nm) | $\lambda_{\text{em}}^b$ (nm) | $\epsilon$ ( $\text{M}^{-1} \text{ cm}^{-1}$ ) | $\Phi^c$ |
|-----------|-------------------------------|------------------------------|--|----------|
| <b>2a</b> | 358, 378, 400, 416            | 446                          | 6404   | 0.67     |
| <b>2b</b> | 350, 368, 404, 426            | 460                          | 5789   | 0.85     |
| <b>2c</b> | 358, 382, 396, 412            | 450                          | 4273   | 0.52     |
| <b>2d</b> | 360, 380, 396, 418            | 448                          | 6620   | 0.64     |
| <b>2e</b> | 352, 376, 400, 414            | 450                          | 5684   | 0.89     |
| <b>2f</b> | 364, 378, 394, 414            | 448                          | 6459   | 0.70     |
| <b>2g</b> | 358, 382, 400, 420            | 458                          | 16 362   | 0.13     |
| <b>2h</b> | 356, 378, 406, 422            | 454                          | 5685   | 0.21     |
| <b>2i</b> | 362, 378, 398, 418            | 454                          | 7284   | 0.12     |
| <b>2k</b> | 382, 396, 420                 | 448                          | 12 844   | 0.20     |
| <b>2l</b> | 356, 376, 396, 416            | 446                          | 6394   | 0.40     |
| <b>2m</b> | 360, 384, 400, 418            | 448                          | 6657   | 0.46     |
| <b>2n</b> | 358, 376, 398, 418            | 450                          | 5133   | 0.64     |
| <b>2o</b> | 360, 378, 398, 418            | 450                          | 4428   | 0.68     |
| <b>2p</b> | 360, 378, 402, 422            | 456                          | 4636   | 0.34     |
| <b>2q</b> | 360, 380, 402, 416            | 456                          | 7473   | 0.30     |
| <b>2r</b> | 370, 388, 408, 428            | 464                          | 10 284   | 0.36     |
| <b>2s</b> | 368, 392, 406, 418            | 466                          | 10 586   | 0.40     |
| <b>2t</b> | 402, 422, 444                 | 486                          | 2333   | 0.26     |
| <b>2u</b> | 372, 386, 408                 | 440                          | 10 226   | 0.33     |
| <b>2v</b> | 400, 420, 438                 | 482                          | 2225   | 0.42     |
| <b>2w</b> | 354, 372, 400, 422            | 450                          | 2487   | 0.79     |
| <b>2x</b> | 358, 376, 398, 418            | 448                          | 4518   | 0.75     |
| <b>2y</b> | 344, 396, 448                 | 562                          | 4880   | 0.43     |

<sup>a</sup> Absorption maxima in DMSO ( $1 \times 10^{-5}$  mol L<sup>-1</sup>). <sup>b</sup> Emission maxima in DMSO ( $1 \times 10^{-5}$  mol L<sup>-1</sup>). <sup>c</sup> Absolute fluorescence quantum yields measured in DMSO ( $5 \times 10^{-6}$  mol L<sup>-1</sup>).

exhibit red-shifts, which may be attributed to the extension of the conjugated system. The exceptional red-shift observed for the diethylamino-containing compound **2y** ( $\lambda_{\text{em}} = 562$  nm) is particularly noteworthy. This pronounced bathochromic effect likely originates from a strong intramolecular charge-transfer interaction between the electron-deficient naphthyridine acceptor and the electron-rich diethylamino (NET<sub>2</sub>) donor, in which the NET<sub>2</sub> is frequently employed in fluorophore to modulate photophysical properties.<sup>17</sup> The tricyclic derivative **2t** and the sulfur-containing tetracyclic compound **2v** also show pronounced red-shifts to 486 nm and 482 nm, respectively. However, the pentacyclic compound **2u** exhibits an emission wavelength similar to that of **2a**. To elucidate the origin of emission wavelength variations among structurally distinct compounds **2a**, **2t**, **2u**, **2v** and **2y**, we performed TD-DFT calculations to determine their adiabatic fluorescence emission energies (Table S2). After optimization and calculation, we found that the adiabatic emission energies of compounds **2a**, **2t**, **2u**, **2v** and **2y** are 3.000, 2.855, 3.032, 2.800 and 2.344 eV, respectively. Consequently, the emission wavelengths are predicted to be longest for compound **2y**, followed by **2t** and **2v** (which exhibit comparable wavelengths), and shortest for **2a** and **2u** (which also show comparable wavelengths). This calculated trend aligns with the experimentally observed fluorescence emission wavelengths discussed earlier, demonstrating that the computational simulations accurately reflect the experimental findings.



To further investigate the influence of different compound structures on fluorescence emission wavelength, we conducted hole–electron analysis (Table 3, Fig. S2). The results revealed that the *D* index for compounds **2a**, **2t**, and **2v** are 0.56 Å, 0.63 Å, and 0.57 Å, respectively, indicating a relatively small spatial separation between the hole and electron centroids. Furthermore, their *Sr* index all reached 0.81, signifying a high degree of overlap between the hole and electron distributions. The corresponding *t* index for these molecules were calculated as –1.48 Å, –1.41 Å, and –1.09 Å, respectively. The significantly negative *t* values, indicating no significant separation between the distributions of holes and electrons, are consistent with a local excitation (LE) character, which consequently results in shorter wavelength emission. Although compound **2u** exhibits a larger *D* index (1.284 Å), its *t* index remains substantially negative (–1.373 Å), also classifying its excitation as LE. In contrast, compound **2y** exhibits a substantially larger *D* index of 2.714 Å, significantly exceeding those of the other molecules. Its *t* index of 0.03 Å indicates significant spatial separation between the hole and electron distributions. As illustrated in Fig. S2, the hole density is not only localized within the  $\pi$ -system but also extends to the diethylamino group. Consequently, the fluorescence excitation in **2y** is characterized as a charge-transfer (CT) excitation. This CT character results in a distinctly red-shifted emission compared to the other compounds.

Next, the absolute fluorescence quantum yields ( $\Phi$ ) of the compounds were measured in DMSO solution ( $5 \times 10^{-6}$  mol L<sup>–1</sup>). Compound **2a** and compounds **2b**–**2f** bearing electron-donating groups exhibit higher absolute fluorescence quantum yields (0.52–0.89) than those with electron-withdrawing groups (**2g**–**2m**; 0.12–0.46). Importantly, compounds **2b** and **2e** exhibit outstanding absolute fluorescence quantum yields of up to 0.89, positioning them as potential candidates for applications as organic small molecular dyes. Furthermore, within the **2n**–**2y** series, the methyl-substituted derivatives **2n** and **2o** exhibit high quantum efficiencies (0.64–0.68). Compounds **2p** and **2q**, containing heavy bromine atoms, exhibit a significant decrease in fluorescence quantum yield (0.30–0.34). The lower fluorescence quantum yields of phenyl-substituted compounds **2r** (0.36) and **2s** (0.40) compared to compound **2a** (0.67) may be attributed to energy dissipation arising from a certain degree of rotational freedom in their molecular structures. Intriguingly, fluorinated derivatives **2w** and **2x** exhibit superior absolute quantum yields (0.75–0.79). Compounds **2v** and **2y** exhibit intermediate absolute fluorescence quantum yields. A modest reduction in

Table 3 Calculated *D*, *Sr* and *t* index of hole–electron analysis

| Compd     | <i>D</i> <sup>a</sup> (Å <sup>–1</sup> ) | <i>Sr</i> <sup>b</sup> /a.u. | <i>t</i> <sup>c</sup> Å <sup>–1</sup> |
|-----------|--|------------------------------|---------------------------------------|
| <b>2a</b> | 0.557                                    | 0.81                         | –1.483                                |
| <b>2t</b> | 0.628                                    | 0.82                         | –1.408                                |
| <b>2u</b> | 1.284                                    | 0.79                         | –1.373                                |
| <b>2v</b> | 0.573                                    | 0.81                         | –1.09                                 |
| <b>2y</b> | 2.714                                    | 0.69                         | 0.03                                  |

<sup>a</sup> Centroid distance index. <sup>b</sup> Overlap index. <sup>c</sup> Separation index.

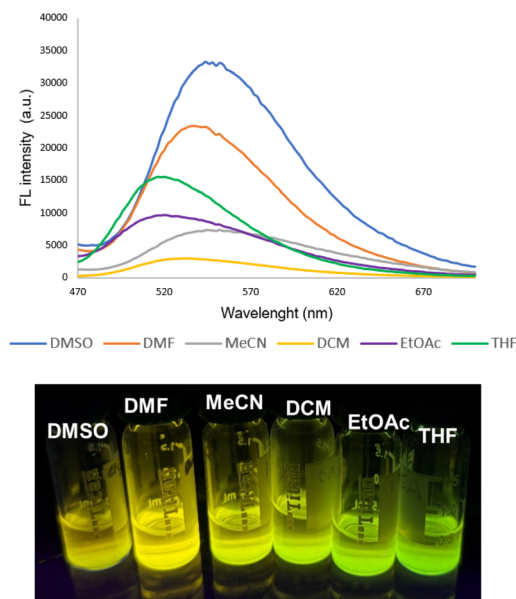


Fig. 2 Solvatochromic effects of compound **2y** excited at 365 nm in different solvents ( $1 \times 10^{-5}$  mol L<sup>–1</sup>).

fluorescence quantum yields is observed for tricyclic system **2t** relative to the pentacyclic analogue **2u**.

Finally, compound **2y**, which is characterised by an intermediate absolute fluorescence quantum yield and a large Stokes shift, was evaluated for solvatochromic behaviour in three classes of solvent: protic (MeOH, EtOH), dipole non-protic (DMSO, DMF, CH<sub>3</sub>CN), and nonpolar (DCM, EA, THF).

As shown in Fig. 2, a pronounced polarity-dependent emission shift with bathochromic displacement was observed in dipole non-protic solvents relative to those in nonpolar media. Interestingly, the fluorescence intensity in protic solvents was markedly quenched (data not shown), likely due to the non-radioactive decay caused by interactions with protic solvents. This polarity-dependent quenching behaviour further suggested the potential as environment-sensitive fluorophore, such as the environment-sensitive reporter.<sup>18</sup>

## Conclusions

We developed a mild and straightforward synthetic strategy to access tri-, tetra-, and pentacyclic 1,6-naphthyridin-4-amine derivatives through CF<sub>3</sub>SO<sub>3</sub>H- or H<sub>2</sub>SO<sub>4</sub>-mediated Friedel–Crafts annulation of 4-(arylamino)nicotinonitrile precursors. The corresponding products were obtained in good to excellent yields (41–98%) within 0.5–4 h. This strategy also proposed a viable approach for late-stage functionalization of 4-(arylamino)nicotinonitrile scaffolds (exemplified by tinib-class kinase inhibitors), which will facilitate further medicinal chemistry research. Additionally, comprehensive photophysical characterisation revealed structure-dependent optical properties, with notable fluorescence performances observed for compounds **2b** and **2e**, which exhibit excellent absolute fluorescence quantum yields of up to 0.89. The NEt<sub>2</sub> group in derivative **2y** appears to



impart an extended Stokes shift while maintaining favourable quantum efficiency, demonstrating a potential modification strategy for developing 1,6-naphthyridin-4-amine-scaffold-based fluorophores with large Stokes shifts. Collectively, the fluorescence characteristics of these compounds exhibit considerable potential for the development of novel organic small-molecule fluorophores.

## Author contributions

Ze Li: data curation, formal analysis, investigation, validation, writing – original draft. Dongfeng Zhang: funding acquisition, writing – review & editing. Hanxun Wang: investigation, writing – original draft. Haihong Huang: project administration, resources, supervision, writing – review & editing. Maosheng Cheng: supervision, project administration. writing – review & editing. Hongyi Zhao: conceptualization, funding acquisition, project administration, supervision, writing – original draft, writing – review & editing.

## Conflicts of interest

The authors declare there are no conflicts of interest.

## Data availability

The data supporting this article have been included as part of the SI.

CCDC 2406765 contains the supplementary crystallographic data for this paper.<sup>19</sup>

Experimental, characterization data, crystallographic data, NMR spectra, absorption spectra, emission spectra and quantum chemical calculations. See DOI: <https://doi.org/10.1039/d5ra03301b>.

## Acknowledgements

We gratefully acknowledge financial support from the National Natural Science Foundation of China (Grant 82103970), and the CAMS Innovation Fund for Medical Sciences (Grant 2021-I2M-1-030).

## Notes and references

- 1 G. Chabowska, E. Barg and A. Wojcicka, *Molecules*, 2021, **26**, 4324.
- 2 M. Lavanya, C. Lin, J. Mao, D. Thirumalai, S. R. Aabaka, X. Yang, J. Mao, Z. Huang and J. Zhao, *Top. Curr. Chem.*, 2021, **379**, 13.
- 3 L. N. Kulikova, G. R. Raesi, D. D. Levickaya, R. Purgatorio, G. Spada, M. Catto, C. D. Altomare and L. G. Voskressensky, *Molecules*, 2023, **28**, 1662.
- 4 J. Fiorito, J. Vendome, F. Saeed, A. Staniszewski, H. Zhang, S. Yan, S. X. Deng, O. Arancio and D. W. Landry, *J. Med. Chem.*, 2017, **60**, 8858–8875.
- 5 H. Wu, W. Wang, F. Liu, E. L. Weisberg, B. Tian, Y. Chen, B. Li, A. Wang, B. Wang, Z. Zhao, D. W. McMillin, C. Hu,

H. Li, J. Wang, Y. Liang, S. J. Buhrlage, J. Liang, J. Liu, G. Yang, J. R. Brown, S. P. Treon, C. S. Mitsiades, J. D. Griffin, Q. Liu and N. S. Gray, *ACS Chem. Biol.*, 2014, **9**, 1086–1091.

- 6 R. A. Kardile, A. P. Sarkate, A. S. Borude, R. S. Mane, D. K. Lokwani, S. V. Tiwari, R. Azad, P. Burra and S. R. Thopate, *Bioorg. Chem.*, 2021, **115**, 105174.
- 7 O. D. Pietro, E. Viayna, E. Vicente-García, M. Bartolini, R. Ramón, J. Juárez-Jiménez, M. V. Clos, B. Pérez, V. Andrisano, F. J. Luque, R. Lavilla and D. Muñoz-Torrero, *Eur. J. Med. Chem.*, 2014, **73**, 141–152.
- 8 M. T. McKenna, G. R. Proctor, L. C. Young and A. L. Harvey, *J. Med. Chem.*, 1997, **40**, 3516–3523.
- 9 H. Li, W. Sun, X. Huang, X. Lu, P. R. Patel, M. Kim, M. J. Orr, R. M. Fisher, T. Q. Tanaka, J. C. McKew, A. Simeonov, P. E. Sanderson, W. Zheng, K. C. Williamson and W. Huang, *ACS Comb. Sci.*, 2017, **19**, 748–754.
- 10 (a) T. A. Palazzo, D. Patra, J. S. Yang, E. E. Khoury, M. G. Appleton, M. J. Haddadin, D. J. Tantillo and M. J. Kurth, *Org. Lett.*, 2015, **17**, 5732–5735; (b) K. Okuma, A. Oba, R. Kuramoto, H. Iwashita, N. Nagahora, K. Shioji, R. Noguchi and M. Fukuda, *Eur. J. Org. Chem.*, 2017, **2017**, 6885–6888; (c) B. S. Arslan, E. Güzel, T. Kaya, V. Durmaz, M. Ke skin, D. Avcı, M. Nebioğlu and İ. Şişman, *Dyes Pigm.*, 2019, **164**, 188–197.
- 11 T. Devadoss, V. Sowmya and R. Bastati, *ChemistrySelect*, 2021, **6**, 3610–3641.
- 12 N. Z. Yalysheva, N. P. Solov'eva, V. V. Chistyakov, Y. N. Sheinker and V. G. Granik, *Chem. Heterocycl. Compd.*, 1986, **22**, 909–914.
- 13 (a) M. Manoj and K. J. R. Prasad, *J. Chem. Res.*, 2009, **2009**, 485–488; (b) M. Manoj and K. J. R. Prasad, *Synth. Commun.*, 2012, **42**, 434–446; (c) E. Okada, M. Hatakenaka, M. Kuratani, T. Mori and T. Ashida, *Heterocycles*, 2014, **88**, 799–806; (d) E. Okada, M. Hatakenaka, Y. Takezawa and K. Iwakuni, *Heterocycles*, 2017, **95**, 322–341.
- 14 (a) W. A. Denny, G. J. Atwell and B. F. Cain, *J. Med. Chem.*, 1977, **20**, 1242–1246; (b) O. G. Backeberg, *J. Chem. Soc.*, 1933, 390–391; (c) W. O. Kermack and N. E. Storey, *J. Chem. Soc.*, 1951, 1389–1392; (d) E. F. Elslager and F. H. Tendick, *J. Med. Chem.*, 1962, **5**, 546–558; (e) A. A. Avetisyan, I. L. Aleksanyan and L. P. Ambartsumyan, *Russ. J. Org. Chem.*, 2005, **41**, 772–773; (f) A. A. Avetisyan, I. L. Aleksanyan and L. P. Ambartsumyan, *Russ. J. Org. Chem.*, 2007, **43**, 1052–1057.
- 15 J. Marco-Contelles, E. Pérez-Mayoral, A. Samadi, M. C. Carreiras and E. Soriano, *Chem. Rev.*, 2009, **109**, 2652–2671.
- 16 (a) M. Janni, A. Thirupathi, S. Arora and S. Peruncheralathan, *Chem. Commun.*, 2017, **53**, 8439–8442; (b) A. Thirupathi, M. Janni and S. Peruncheralathan, *J. Org. Chem.*, 2018, **83**, 8668–8678; (c) D. Bandyopadhyay, A. Thirupathi, D. Radhakrishnan, A. Panigrahi and S. Peruncheralathan, *Org. Biomol. Chem.*, 2021, **19**, 8544–8553; (d) P. Iniyavan, A. Avadhani, Y. Kumar, A. S. J. Chakravarthy, M. A. Palluruthiyil and H. Ila, *J. Heterocycl. Chem.*, 2022, **59**, 2240–2257; (e) Guilin Medical



University, *CN Pat.*, ZL201910698398.3, 2019; (f) Guilin Medical University, *CN Pat.*, ZL202110536683.2, 2021.

17 (a) G. Jiang, T. B. Ren, E. D'Este, M. Xiong, B. Xiong, K. Johnsson, X. B. Zhang, L. Wang and L. Yuan, *Nat. Commun.*, 2022, **13**, 2264; (b) D. Insuasty, M. Mutis, J. Trilleras, L. A. Illicachi, J. D. Rodríguez, A. Ramos-Hernández, H. G. San-Juan-Vergara, C. Cadena-Cruz, J. R. Mora, J. L. Paz, M. Méndez-López, E. G. Pérez, M. E. Aliaga, J. Valencia and E. Márquez, *ACS Omega*, 2024, **9**, 18786–18800.

18 T. Li, Q. Y. Zong, H. Dong, I. Ullah, Z. H. Pan and Y. Y. Yuan, *Nat. Commun.*, 2025, **16**, 1892.

19 Z. Li, D. Zhang, H. Wang, H. Huang, M. Cheng and H. Zhao, Mild synthesis of fused polycyclic 1,6-naphthyridin-4-amines and their optical properties, (CDDC [2406765]: Experimental CrystalStructure Determination), 2024, DOI: [10.5517/ccde.csd.cc2lsflf](https://doi.org/10.5517/ccde.csd.cc2lsflf).

